Optimization Methods for Thermal Modeling of Optomechanical Systems

Miltiadis V. Papalexandris , Mark H. Milman, and Marie Levine

Jet Propulsion Laboratory,
California Institute of Technology,
Pasadena, CA 91109

ABSTRACT

Numerical techniques for a class of optimization problems associated with the thermal modeling of optomechanical systems are presented. Emphasis is placed on applications where radiation plays a dominant role. This work is motivated by the need of incorporating thermal analysis into integrated modeling of high-precision, space-borne optical systems. The specific problems of interest are the thermal control (whose objective is the minimization of the wavefront error or the elimination of temperature variations via application of external heat loads), and the temperature estimation problem (whose objective is the prediction of temperatures at arbitrary nodes of the model, given noisy measurements on a subset of nodes). The proposed numerical techniques are briefly described and compared to exisiting algorithms. Their accuracy and robustness are demonstrated through numerical tests with models from onoging NASA missions.

Keywords: thermal networks, thermal control, estimation, optomechanical design, space telescopes.

1. INTRODUCTION

Thermal modeling and heat-transfer analysis is a critical part in the design of many engineering applications. The various numerical techniques that have been developed over the years for this purpose can be divided in two main categories; finite-element and finite-difference techniques. They are both derived from discretizations of the underlying heat-transfer equation. Among them, one of the most popular techniques is the thermal network (or lumped-parameter) approach. This approach is derived from a particular finite-difference discretization of the governing equation. According to this method, the system is partitioned to isothermal nodes with pointwise properties that can exchange heat either by conduction or radiation. The main advantages of the thermal network approach are flexibility and straightforward implementation of components with complicated geometry.

Accurate thermal modeling is also considered an important part of integrated modeling, a methodology where multidisciplinary models are developed for the design and analysis of engineering systems. It is emerging as an indispensable tool in modern engineering practice because it simplifies and speeds up the analysis of very complicated systems. Furthermore, it allows the study of various internal and external factors, and their impact on the system of interest, even during the early design stages. Spacecrafts and space-born science instruments, along with many other aerospace applications, are typical examples of systems with high demand for integrated modeling.

The present work is motivated from the need of incorporating thermal analysis into integrated modeling of high-precision, space optical systems. More specifically, it is concerned with the three fundamental aspects of optimization and control of steady-state thermal network models. The objective of active control is to achieve a desired temperature profile via addition or subtraction of heat. On the other hand, the objective of node-updating is the estimation of temperatures at locations where direct measurements can not be made due to physical and economic constraints. The importance of these aspects of thermal modelling has increased in recent years due to high precision and stability requirements of modern applications.

2. DESCRIPTION OF THERMAL NETWORKS

This section is devoted to a brief description of the thermal network equations. The following definitions are necessary for the discussion that follows. Let $\mathbb{R}^N$ be the real, N-dimensional linear space of column vectors $x = [x_1, \ldots, x_N]^{\mathrm{T}}$. The coordinate-wise partial ordering on $\mathbb{R}^N$ implies that if $x, y \in \mathbb{R}^N$, then $x \geq y$ if and only if $x_i \geq y_i$ for all $i = 1, \ldots, N$. The Euclidean norm $|x| = \{\sum_{i=1}^{N} x_i^2\}^{1/2}$ in $\mathbb{R}^N$ will also be used. Finally, let $\mathbb{R}^N_+ = \{x \in \mathbb{R}^N : x \geq 0\}$.

A thermal network is defined by a set of nodes that are connected to each other via linear or quartic conductances, Holman (1997), Birkhoff & Kellogg (1966). It is analogous to electrical networks. In principle, a thermal network model arises from a finite-difference discretization of the steady-state, heat-transfer equation,

$$\nabla \cdot (k \nabla T) \; = \; f \,, \tag{1}$$

where k is the thermal conductivity, T is the temperature, and f is the heat load. In many occasions, however, the network approach is adopted to construct models of complex systems in which a node is merely an isothermal component and is not derived directly from discretization of equation (1).

In general, a thermal network model consists of N internal nodes and n boundary nodes. The temperature distribution on the boundary is assumed to be known and given. The finite-difference discretization of (1) reduces to the following set of N nonlinear algebraic equations,

$$\hat{Q}_i + \sum_{j=1}^{N+n} \hat{C}_{ij}(T_j - T_i) + \sum_{j=1}^{N+n} \hat{R}_{ij}(T_j^4 - T_i^4) \; = \; 0 \,, \quad i = 1, \ldots, N \,. \tag{2}$$

In the above equations, $\hat{Q}_i$ are the heat loads of the system, while $\hat{C}_{ij}$ and $\hat{R}_{ij}$ are the conduction and radiation coefficients of the system, respectively.

The conduction coefficients are given by Fourier's law,

$$\hat{C}_{ij} \; = \; \frac{kA}{L} \,, \tag{3}$$

where k is the thermal conductivity of the material (it can be either constant or temperature dependent), A is the cross-sectional area of heat flow, and L is the length between nodes i and j. Convection conductors are computed from the expression

$$\hat{C}_{ij} \; = \; hA \,, \tag{4}$$

where h is the convective heat transfer coefficient and A is the surface area in contact with the fluid. On the other hand, the radiation coefficients are given by

$$\hat{R}_{ij} \; = \; \sigma \, A \, \varepsilon \,, \tag{5}$$

where σ is the Stephan-Boltzmann constant, A is the area that corresponds to node i, and ε is the emissivity between nodes i and j.

The system (2) can be written as a matrix equation after the following substitutions. First, let $T = [T_1, \ldots, T_N]^{\mathrm{T}}$ and $D(T) = [T_1^4, \ldots, T_N^4]^{\mathrm{T}}$. Further, define the $N \times N$ matrices C and R as

$$C_{ij} = \left\{ \begin{array}{ll} \hat{C}_{ij}, & \text{if } i \neq j, \\ -\sum_{j=1}^{N+n} \hat{C}_{ij}, & \text{if } i = j. \end{array} \right\} \,, \qquad R_{ij} = \left\{ \begin{array}{ll} \hat{R}_{ij}, & \text{if } i \neq j, \\ -\sum_{j=1}^{N+n} \hat{R}_{ij}, & \text{if } i = j. \end{array} \right\} \tag{6}$$

Finally, let $Q = [Q_1, \ldots, Q_N]^{\mathrm{T}}$ be the forcing vector of the system (2), arising from the combination of the heat loads $\hat{Q}_i$, and the energy exchange through the boundary nodes. In other words,

$$Q_i \;=\; \hat{Q}_i + \tilde{Q}_i\,, \qquad i = 1, \ldots, N\,, \tag{7}$$

with

$$\tilde{Q}_i \;=\; \sum_{j=N+1}^{N+n} \hat{C}_{ij} T_j \;+\; \sum_{j=N+1}^{N+n} \hat{R}_{ij} T_j^4\,, \qquad i = 1, \ldots, N\,. \tag{8}$$

After making these substitutions, the thermal network equation (2) is written in the more compact form

$$F(T) \;\equiv\; Q + CT + RD(T) \;=\; 0\,. \tag{9}$$

3. ACTIVE CONTROL FOR THERMAL NETWORKS

Suppose that there are $M \leq N$ nodes in the system (9) whose temperatures have to be controlled. For simplicity assume that these are the first M nodes of the system and denote by $T_\alpha \in I\!R_+^M$ their temperature vector. Also, denote by T_β the temperatures of the remaining nodes, *i.e.*, $T = [T_\alpha, T_\beta]$. Also, consider a target (*i.e.*, measured) temperature profile $T_0 \in I\!R_+^M$ and a least-square type objective function w associated with T_α,

$$w(T_\alpha) \;=\; (T_\alpha - T_0)^{\mathrm{T}} \cdot E \cdot (T_\alpha - T_0)\,. \tag{10}$$

The temperature vector T must satisfy the thermal network equation (9). More specifically, T_α is the solution vector of the first M equations of the network. In the above equation, E is an $M \times M$ constant, positive definite matrix. Typically, w represents a physical quantity of interest that is directly associated to the performance of the system. The matrix E represents the functional relation of the performance index with the temperature distribution. In imaging systems, w is the wavefront error of the system and E depends on the thermal, structural and optical characteristics of the system.

The purpose of thermal control is to achieve a distribution T_α such that w attains a minimum. The control action is provided by thermal loads applied to $M_1 \leq N$ nodes. In other words, the control vector consists of the M_1 non-zero elements of $\hat{Q} \in I\!R^N$. Therefore, the active control problem is formulated as a nonlinear, least-squares minimization problem with constraints with respect to the objective function w as follows.

$$\min_{\hat{Q}} w(\hat{Q}) \;=\; \Big(T_\alpha(\hat{Q}) - T_0\Big)^{\mathrm{T}} \cdot E \cdot \Big(T_\alpha(\hat{Q}) - T_0\Big)\,, \tag{11}$$

subject to the following $M_2 = 2(M_1 + 1)$ constraints:

$$\begin{aligned} b_i^{\mathrm{L}} \;&\leq\; \hat{Q}_i \;\leq\; b_i^{\mathrm{U}}\,, \qquad i = 1, \ldots, M_1\,, \\ \hat{Q}_{\mathrm{MIN}} \;&\leq\; \sum_{i=1}^{M_1} \hat{Q}_i \;\leq\; \hat{Q}_{\mathrm{MAX}}\,, \end{aligned} \tag{12}$$

where $\sum b_i^{\mathrm{L}} \leq \hat{Q}_{\mathrm{MIN}}$ and $\hat{Q}_{\mathrm{MAX}} \leq \sum b_i^{\mathrm{U}}$. The above constraints express practical limitations in the available power that can be produced by the heaters or coolers of the system. The temperature vector $T_\alpha(\hat{Q})$ appearing in (11) is the solution of the first M equations of the thermal network equations (9) and, therefore, is a function of the heat-load vector $\hat{Q}$. It is common practice to place the controllers on nodes whose temperature have to be regulated. This is the case of the *collocated control problem.*

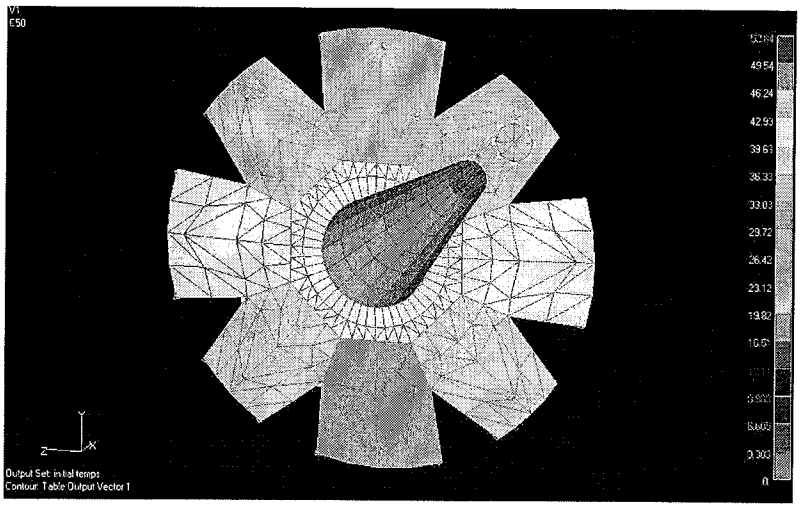

Figure 1. Schematic of the NGST thermal model and initial temperature distribution.

The above system of equations is an example of constrained, nonlinear optimization problem. The proposed algorithm for solving this system is based on the Sequential Quadratic Programming method (SQP) method, Han (1977) and Powell (1978), and a recently developed thermal network solver, Milman & Petrick (2000). Details of the algorithm can be found in Papalexandris & Milman (2001). The SQP method is one of the most popular methods for nonlinear optimization problems due to its robustness and good convergence properties. It is based on an iterative procedure where a quadratic programming subproblem with linearized constraints is solved during each step, thus generating a sequence of approximations to the solution. On the other hand, the steady-state thermal solver relies on a restricted stepsize Newton method. The Newton iterates are evaluated along a descent direction for $|F(T)|^2$. The stepsize of each iteration is determined via a back-tracking line-search procedure, Dennis & Schnabel (1987). A useful feature of the proposed thermal control algorithm is the analytic (in case of constant heat-transfer coefficient), or semi-analytic (otherwise) evaluation of the Jacobian of the thermal network, $\partial F/\partial T$, and the gradient of the object function, w. The elimination of finite-differencing procedures for evaluation of derivatives dramatically accelerates the convergence rate of the algorithm and offers significant computing-time savings.

The proposed algorithm has been applied to a network model of a proposed design for the Next Generation Space Telescope (NGST), shown in Figure 1. This model was prepared by the NASA Goddard and NASA Marshall Space Centers. The most significant heat load applied on the telescope is radiation from the sun and the earth. The amount of radiation varies considerably as the telescope rotates to aim at different parts of the sky. Non-negligible temperature variations (a few degrees Kelvin) on the components of the instrument are experienced, even with the presence of sunshields. Every deviation of the temperature profile from the nominal configuration generates thermal stresses that cause deformations of the surfaces of the primary and secondary mirrors of the telescope. In turn, these deformations produce aberrations that may degrade the performance of the instrument. The effects of thermal stresses can be minimized with the employment of a suitable control strategy.

The objectives of the control strategy depend on the information available about the instrument. For example, one objective is to maintain the initial temperature distribution. Another possible objective is to achieve optimal performance of the instrument making use of the knowledge of the wavefront. Two different objective functions have been used in the present study. The first one is the norm of the temperature change. In other words, the matrix E of equation (16) is the identity matrix, *i.e.*, $E = I$. This case is referred to as *temperature control.* The second performance index is the wavefront error (WFE) of the telescope. The wavefront error is a measure of the performance of the telescope and is defined below. This case is

referred to as *WFE control.*

Under the assumption of the validity of linear theories, the deformations ξ induced by temperature changes on m nodes satisfy the following linear system,

$$K \cdot \xi \;=\; W \cdot (T_\alpha - T_0)\,, \tag{13}$$

where K is the stiffness matrix of the structure, W is the temperature-to-stress transformation matrix, and T_0 is the vector of the nominal, zeros-stress temperatures of the m nodes of interest.

The stiffness matrix K is singular due to degrees of freedom that correspond to rigid-body motion. These singularities can be removed by specifying single-point constraints. This procedure results in a new, symmetric and invertible matrix, $\tilde{K}$. The solution to the above system, ξ, is computed via Cholesky decomposition of $\tilde{K}$.

The Optical Path Difference vector of the telescope, (OPD), is defined as

$$OPD \;=\; O \cdot \xi\,, \tag{14}$$

where O is the matrix of optical sensitivity to deformations for the system. Finally, the wavefront error is defined as

$$w \;=\; (T_\alpha - T_0)^{\mathrm{T}} \cdot E \cdot (T_\alpha - T_0) \;+\; w_0\,, \tag{15}$$

with E given by

$$E \;=\; \left(O \cdot \tilde{K}^{-1} \cdot W\right)^{\mathrm{T}} \cdot \left(O \cdot \tilde{K}^{-1} \cdot W\right)\,. \tag{16}$$

Since subtraction of heat requires expensive and complicated instrumentation, the telescope is assumed to operate at a nominal, 'hot' position, so that any rotation causes the temperatures to drop. Then, the desired temperature profile can be restored by adding heat to the system. Before applying the desired control strategy, the location of the heaters has to be determined. Since a node of a thermal network corresponds to an actual isothermal component of the system, the selection of the location of the controllers reduces to determining which M_1 components of the N-dimensional heat-load vector $\hat{Q}$ will be non-zero. This selection can be performed by some suitable ranking of the importance of the N available locations with respect to the performance index.

More specifically, one observes that the objective function (11) depends directly only on the M nodes that T_α consists of, and not on all the N nodes of the network. Therefore, it is natural to assume that these M nodes have higher priority over the rest. Further, the M most important nodes can be ranked via the following procedure. First, the eigenvalues, e_i, and left eigenvectors v_i, $i = 1, \ldots, m$ of the $m \times m$ matrix E. equation (16), are computed. Then, the vector V, defined as

$$V \;=\; \sum_{i=1}^{m} e_i \cdot v_i\,. \tag{17}$$

is computed. The elements of V are subsequently ranked according to their absolute values. This ranking gives a measure of the relative importance of the M nodes to the index w. Heaters are then placed on the first M_1 nodes of this ranking.

If $M_1 \leq M$, which is the case most often encountered in practice, then the top M_1 nodes of the ranking determine the locations where heaters will be applied. In the unlikely case of $M_1 > M$, then all the M of T_α get a controller. The rest $M_1 - M$ controllers can either be placed on the nodes that conduct the most with the top-ranked nodes of T_α, or may not be used at all. This empirical procedure is quite general and

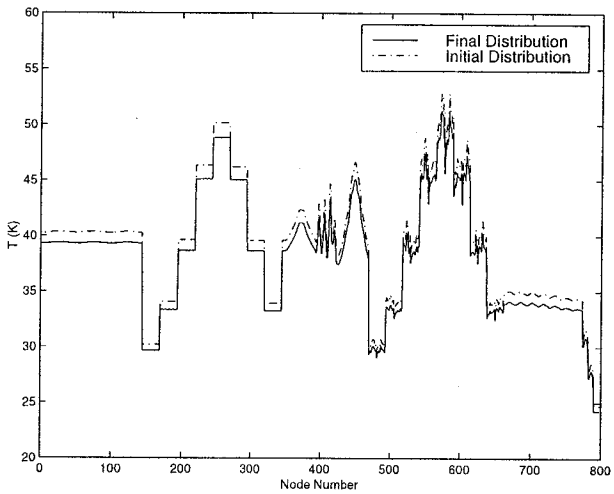

Figure 2. Initial and final (without control) temperature distributions.

can be applied whenever the heater locations are not known *a priori*. The eigenvalues and eigenvectors of E can be computed quite accurately with standard algorithms. Therefore, this procedure can be easily implemented. On the other hand, if the properties of the structure are such that the eigenvalues of E are not well spaced, the ranking might be sensitive to perturbations of E, *e.g*, the relative weight of some nodes might change.

The goal, however, is to identify a suitable *group* of nodes where heaters will be located (and usually there are no strict limits on the number of heaters that will be used). The proposed procedure is not intended to be used as the absolute criterion for selecting the nodes where heat will be applied, but it is expected to yield reasonable results so that it can supplement good engineering judgement. Even if the node-ranking undergoes small or moderate changes, the group that is selected from this procedure will still include most of the important nodes.

The thermal model of NGST consists of $N = 1802$ internal nodes and $n = 48$ boundary nodes. There are more than 5800 linear conductors and more than 160,000 radiation conductors. Furthermore, there are $M = 798$ nodes whose temperature has to be controlled. These are the internal nodes that are used to model the primary mirror of the telescope. When the instrument rotates from the 'hot' position, the temperature drops by a couple of degrees Kelvin. The induced thermal stresses generate a wavefront error equal to 107.58 nm. The initial and final (without control) profiles are plotted in Figure 2.

There are $M_1 = 100$ heaters available for thermal control. The maximum available power is set at $Q_{\text{MAX}} = 0.5$ W. First the locations of the heaters are selected via the above procedure and subsequently the heat output from each heater is determined. As mentioned above, the goal of temperature control is to apply heat so that the final distribution is as close as possible to the initial (hot) distribution. Similarly, the goal of WFE control is to apply heat to minimize the wavefront error (15) directly.

Application of temperature control produces a profile that is very close to the initial, 'hot', configuration, Figure 2. The required energy output from the heaters is 0.20 W. The final WFE after temperature control is reduced to 27.62 nm. On the other, hand WFE control results in a temperature profile that is very close to the 'cold' (without-control) profile, Figure 3. The required energy output is only 0.007 W, about 1/30 of the required energy for temperature control. The wavefront error after WFE control is 27.78 nm, just slightly higher than the error after temperature control. The power output that is required from each heater is presented in Figure 3 for both control strategies. Finally, gray plots of the Optical Path Difference

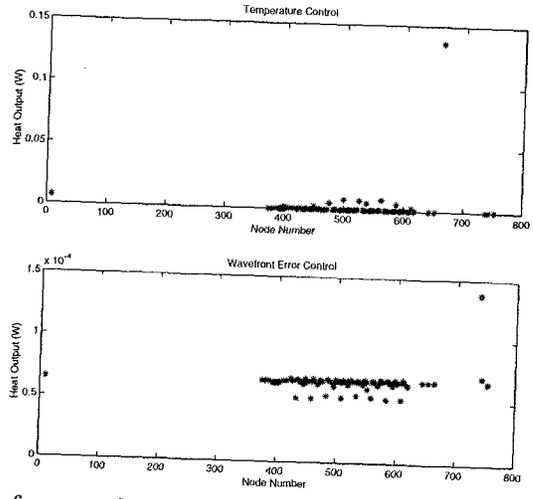

Figure 3. Heat output from each heater after temperature and wavefront error control.

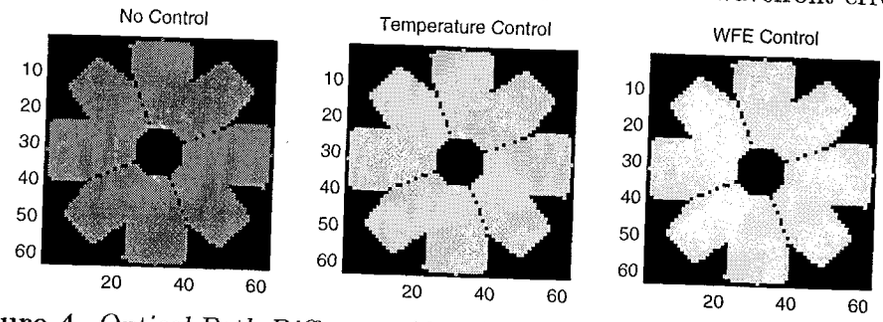

Figure 4. Optical Path Difference (OPD) without control and after control.

(OPD) with and without thermal control are shown in Figure 4. It can be observed that the OPD has been significantly reduced after employing the two proposed control strategies.

To explore the difference in the value of the wavefront error between the two control strategies, further numerical tests were performed. The final temperature profile and heat loads after temperature control were used as a new initial condition for WFE control. The algorithm converged to a temperature distribution that was very close to this new initial condition, requiring just an additional heat output of 0.01 W. The wavefront error, however, was reduced to a value of 16.3 nm. This value represents another local minimum of WFE as defined in (15).

4. TEMPERATURE ESTIMATION FOR THERMAL NETWORKS

This section is devoted to the temperature estimation problem of thermal networks. Assume that temperature measurements can be taken at M nodes of the network. These are the *observable* nodes of the system, denoted as the α set. The remaining $N - M$ nodes are the *unobservable* nodes of the system, denoted as the β set. Let $\hat{T}$ denote the set of measured temperatures at the observable nodes. Finally, assume that the nodes of the system have been rearranged so that the temperature vector T can be partitioned as $T = [T_\alpha, T_\beta]$, where T_α is the temperature vector of the α set, and T_β is the temperature vector of the β set. Then the system (9) can be partitioned as

$$\begin{bmatrix} F_1(T_\alpha, T_\beta) \\ F_2(T_\alpha, T_\beta) \end{bmatrix} = \begin{bmatrix} Q_\alpha \\ Q_\beta \end{bmatrix} + \begin{bmatrix} C_{\alpha\alpha} & C_{\alpha\beta} \\ C_{\beta\alpha} & C_{\beta\beta} \end{bmatrix} \begin{bmatrix} T_\alpha \\ T_\beta \end{bmatrix} + \begin{bmatrix} R_{\alpha\alpha} & R_{\alpha\beta} \\ R_{\beta\alpha} & R_{\beta\beta} \end{bmatrix} \begin{bmatrix} D(T_\alpha) \\ D(T_\beta) \end{bmatrix} = \begin{bmatrix} 0 \\ 0 \end{bmatrix}, \qquad (18)$$

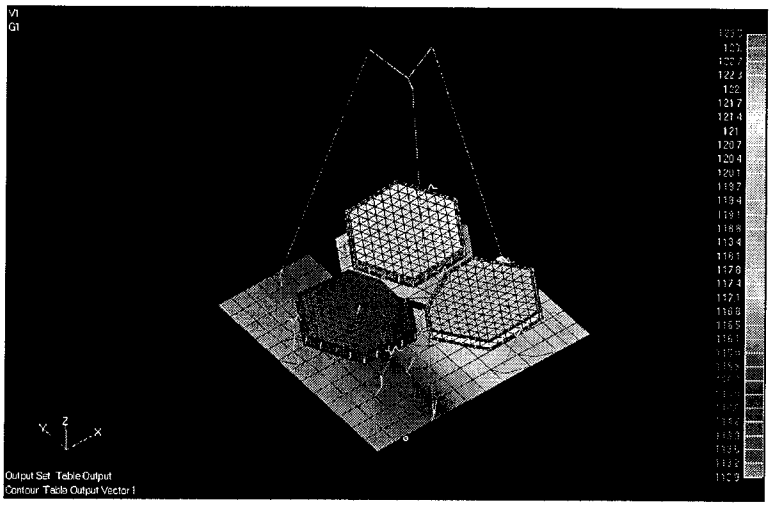

Figure 5. Schematic of the spacecraft thermal model and initial temperature distribution.

where $C_{\alpha\alpha}$, $R_{\alpha\alpha}$ are the $M \times M$ principal sub-matrices of C and R, while $C_{\beta\beta}$ and $R_{\beta\beta}$ are $(N-M) \times (N-M)$ sub-matrices of C and R, respectively.

The approach to producing estimates for the temperature profiles at the unobservable nodes is to add artificial (fictitious) heat loads to the observed nodes of the network so that the solution to the equations at the observed nodes are within the measurement error. For example, if zero measurement error is assumed, then the goal is to introduce new forcing terms to the observed nodes so that the solution to the network equations at those nodes equals the measured values. The underlying idea behind this approach is that all the thermal parameters of the model are correct except possibly the explicit heat loads. Therefore, any deviation of the computed observed temperatures from the measured ones can be corrected by adding artificial heat loads to the original system.

Obviously, the artificial heat-load vector that modifies the governing equation in the manner described above is not unique. It is natural, however, to select the vector with the minimum norm because this vector represents the smallest external disturbance to the system. Then, the temperature estimation problem can be formulated as a nonlinear, least-squares minimization problem for the l_2-norm of the artificial forcing vector:

$$\min_T |F_1(T)|^2 , \tag{19}$$

cf (20), subject to

$$F_2(T) = 0 , \tag{20}$$

$$|T_\alpha - \hat{T}|^2 \leq \epsilon |\hat{T}|^2 . \tag{21}$$

Numerical experiments showed that SQP-based algorithms for this problem become too slow when the number of unobservable nodes becomes large (> 1000). It is, therefore, desired to develop an alternative method with improved speed for the solutions of the problems of interest.

The proposed algorithm for the temperature estimation problem is a Gauss-Newton iterative procedure which takes advantage of the particular structure of the above equations. In particular, we exploit the fact that, on each iteration step, the (linearized) version of (20) can easily be solved to produce an expression of the form $T_\beta = f(T_\alpha)$. This expression can be substituted to the (linearized) version of (19) to obtain an iterate for the objective function that depends on T_α only.

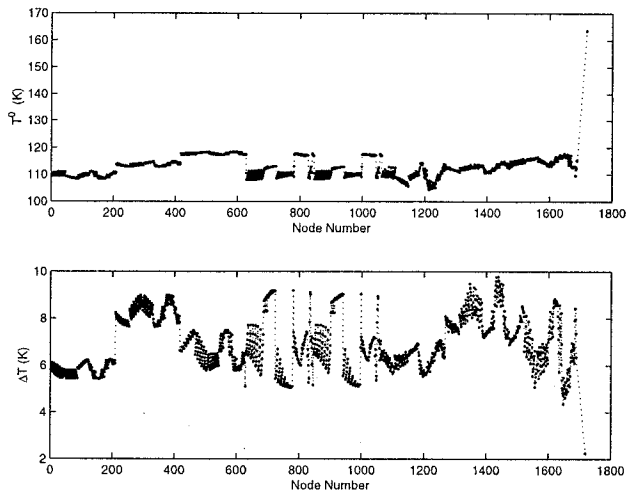

Figure 6. Upper part: initial temperature distribution. Lower part: difference between target (hot) and initial (cold) temperature distributions.

This objective-function iterate is subject to a single quadratic constraint for the vector T_α. Therefore, on each iteration step we have to solve a least-squares problem with a single quadratic constraint (LSQI). Traditional techniques for the LSQI problem employ Singular Value Decomposition (SVD) which is a slow procedure. In order to improve the speed of the optimization process, a new numerical method for the LSQI problem has been developed, Papalexandris *et al* (2001). This newly developed LSQI solver is based on QR decomposition instead of SVD and produces significant computational savings.

The proposed Gauss-Newton procedure method has been applied to the thermal model of a proposed NASA flight experiment. This experiment was designed to demonstrate the feasibility of technology for large-size, segmented, space telescopes, such as the next generation space telescope (NGST). The primary mirror of the telescope consists of three segments. Passive thermal control is provided by the sun-shield, located in the back of the primary mirror. A schematic of the thermal model, along with a plot of the initial thermal distribution is shown in Figure 5.

The thermal model of the spacecraft consists of $N = 1689$ interior nodes, $n = 30$ boundary nodes, 5153 linear and 100417 quartic (radiation) conductors. The temperature at the boundary nodes is time dependent. For the purposes of the present study, the cold temperature distribution is considered to be the profile initially computed by the thermal model. The hot distribution is the target, 'measured', profile that must be predicted by the proposed algorithms. The initial profile and its difference from the target are plotted in Figure 6. It should be mentioned that this difference is quite large (it can be as high as $10\,K$) and it is used only to test the efficiency of the proposed algorithm in extreme conditions.

Further, it is assumed that there were sensors available at $M = 100$ nodes. Sometimes various design considerations impose constraints on the possible location of the temperature sensors. In this test case, it was assumed that there were no such restrictions and the sensors were placed in the most *important* locations with respect to deformations of the primary mirror. This means that the interior nodes of the system had be ranked according to their effect on the deformations of interest. This ranking can be accomplished via the following semi-empirical procedure.

Assume that there are M_1 nodes that are important for the optical performance of the telescope. Under the assumption of linearity, the deformations ξ induced by temperature changes are given by satisfy the following linear system,

$$\xi \;=\; K^{\dagger} W \cdot (T - T_0)\,, \tag{22}$$

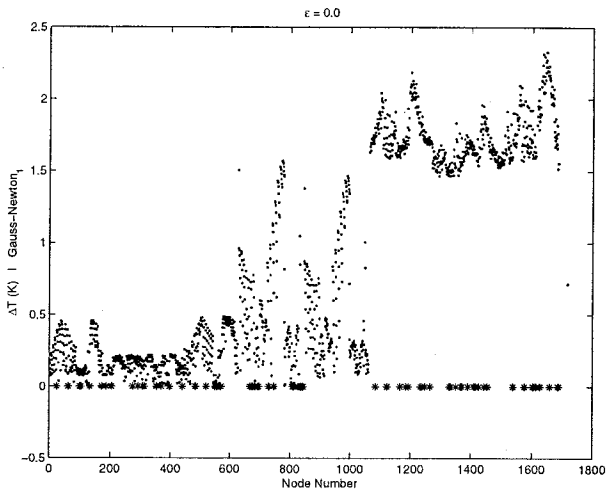

Figure 7. Difference between target and predicted temperature distributions. Tolerance, $\epsilon = 0$.

where $K^{\dagger}$ is the pseudo-inverse of the stiffness matrix K, W is the temperature-to-stress transformation matrix, and T_0 is the vector of the nominal, zeros-stress temperatures of the nodes of interest. Consider the sub-matrix consisting of the rows of the product $K^{\dagger}W$ that correspond to the elements of ξ that are interesting, and determine its singular values and singular vectors, say e_i and v_i, $i = 1, \ldots, M_1$, respectively. Once the singular values and vectors have been computed, the vector V defined as

$$V = \sum_{i=1}^{m} e_i \cdot v_i \,, \tag{23}$$

is formed. Next, the elements of V are ranked according to their absolute values. This ranking gives a measure of the relative importance of the nodes of the system to the M_1 deformations of interest.

In the present example, there are $M = 100$ observable nodes. The deformations of interest are the three translational displacements of each node in the model the primary mirror. The structural grid for the mirror consists of 627 points. Therefore, the number of deformations of interest is $M_1 = 627 \times 3 = 1881$. The above semi-empirical procedure is employed for the determination of the observable nodes. Approximately one third of them are located at the primary mirror, another third at the backplane, and the other third at the bench.

The proposed Gauss-Newton algorithm has been applied for the estimation of the temperature at the unobserved nodes. The error of the proposed method when $\epsilon = 0$ is shown in Figure 7. In particular, the maximum pointwise error was less than $2.5\,K$. This result is very satisfacotry considering that the observablable nodes make up just a small fraction ($< 6\%$) of the interior nodes. Subsequently, ϵ assumed a value of 7×10^{-5}, which corresponds to an average measurement error of $1.02\ K$. In practice, of course, temperature measurement errors are much smaller. The objective of this numerical experiment, however, was to test the robustness of the proposed algorithm and explore its accuracy under severe constraints. The error on the estimated temperatures is shown in Figure 8. The maximum pointwise error was about $8\,K$. This simply implies that if the quality of the measurements does not improve, more measurements must be made in order to achieve better accuracy in the prediction.

5. CONCLUSIONS

The present study was focused on two optimization problems that frequently arise in thermal modeling of optomechanical systems, These problems are active thermal control and temperature estimation. Both of

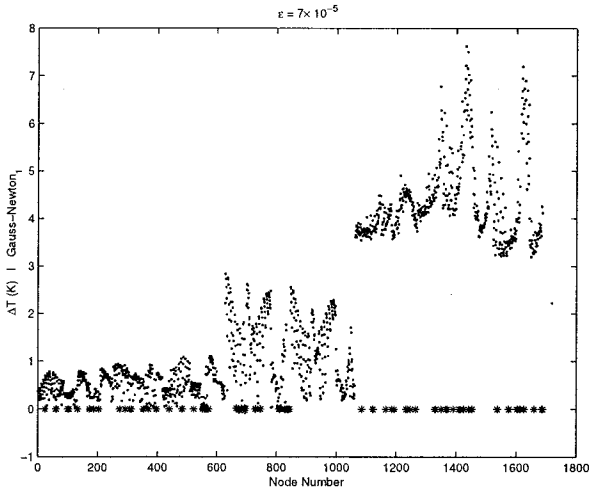

Figure 8. Difference between target and predicted temperature distributions. Tolerance, $\epsilon = 7 \times 10^{-5}$.

them are formulated as nonlinear, constrained optimization problems. The proposed numerical procedure for thermal control is based on the SQP method and a newly developed thermal-network solver, and employs analytical or semi-analytical evaluation of the Jacobian of the objective functions. It has been tested on large-scale thermal models of space telescopes with quite promising results as regards both their accuracy and their convergence rate.

For the temperature estimation problem, however, the SQP method becomes too slow, when the number of unknown temperatures is large (> 1000, approximately). For this reason, a Gauss-Newton iterative procedure was proposed, tailored to the particular structure of the estimation problem. During each iteration step an LSQI problem is solved via a newly-developed solver that combines speed with robustness. The algorithm was tested on a large-scale thermal model of a proposed space-telescope concept with satisfactory results.

ACKNOWLEDGMENTS

This work was prepared at the Jet Propulsion Laboratory, California Institute of Technology, under a contract with National Aeronautics and Space Administration.

REFERENCES

[] J.P. Holman, *Heat Transfer*, 8th edition, Mc Graw Hill, New York, 1997.

[] S.P. Han, "A globally convergent method for nonlinear programming," *J. Opt. Th. Appl.*, **22**, p. 297, 1977

[] M.J.D. Powell, "Algorithm for nonninearly constrained optimization calculations," *Numerical Analysis*, **630**, Springer Verlag, Berlin, 1978.

[] M.H. Milman, and W. Petrick, "A note on the solution to a common thermal network problem encountered in heat transfer analysis of spacecraft," *Appl. Math. Model.*,**24**, pp. 861-879, 2000.

[] M.V. Papalexandris, and M.H. Milman, "Active Control and Parameter Updating Techniques for Nonlinear Thermal Network Models," *Comp. Mech.*, Vol. **27**, pp. 11-22, 2001.

[] J.E. Dennis, and R.B. Schnabel R, *Numerical Methods for Unconstrained Optimization and Nonlinear equations*, SIAM, Philadelphia, PA, 1996.

[] M.V. Papalexandris, M.H. Milman, and M.B. Levine, "Node-Prediction Algorithms for Nonlinear Thermal Network Models," *AIAA J.*, submitted, 2001.